Increased oxidative stress precedes the onset of high-fat diet-induced insulin resistance and obesity

Increased oxidative stress precedes the onset of high-fat diet-induced insulin resistance and obesity

Naoto Matsuzawa-Nagata [1, 2], Toshinari Takamura [2], Hitoshi Ando [2], Seiji Nakamura [1, 2], Seiichiro Kurita [2], Hirofumi Misu [2], Tsuguhito Ota [2], Masayoshi Yokoyama [2], Masao Honda [2], Ken-ichi Miyamoto [1], Shuichi Kaneko [2]

[1] Department of Medicinal Informatics and [2] Department of Disease Control and Homeostasis, Kanazawa University Graduate School of Medical Science, Kanazawa, Japan

Corresponding author: Toshinari Takamura, MD, PhD, Department of Disease Control and Homeostasis, Kanazawa University Graduate School of Medical Science, 13-1 Takara-machi, Kanazawa, Ishikawa 920-8641, Japan, Tel:+81-76-265-2233, Fax:+81-76-234-4250, E-mail: ttakamura@m-kanazawa.jp

Running title: oxidative stress induced by high-fat diet

Key words: insulin resistance, oxidative stress, β-oxidation, NADPH oxidase

Reprint requests to corresponding author.

The abbreviations used are the following: HFD, high-fat diet; ROS, reactive oxygen species; PPARα, peroxisome proliferator-activated receptor-α; Nox, NADPH oxidase; FFAs, free fatty acids; Acox, acyl-CoA oxidase; CPT-1a, carnitine palmitoyltransferase 1a; CYP2E1, cytochrome P450 2E1; GTT, glucose tolerance test; Gpx, glutathione peroxidase; ITT, insulin tolerance test.

Abstract

Insulin resistance is a key pathophysiological feature of metabolic syndrome. However, the initial events triggering the development of insulin resistance and its causal relations with dysregulation of glucose and fatty acids metabolism remain unclear. We investigated biological pathways that have the potential to induce insulin resistance in mice fed a high-fat diet (HFD). We demonstrate that the pathways for reactive oxygen species (ROS) production and oxidative stress are coordinately up-regulated in both the liver and adipose tissue of mice fed a HFD prior to the onset of insulin resistance through discrete mechanism. In the liver, a HFD up-regulated genes involved in sterol regulatory element binding protein-1c (SREBP-1c)-related fatty acid synthesis and peroxisome proliferator-activated receptor-α (PPARα)-related fatty acid oxidation. In the adipose tissue, however, the HFD down-regulated genes involved in fatty acid synthesis and up-regulated NADPH oxidase (Nox) complex. Furthermore, increased ROS production preceded the elevation of TNF-α and free fatty acids (FFAs) in the plasma and liver. ROS may be an initial key event triggering HFD-induced insulin resistance.

Key words: Insulin resistance; obesity; reactive oxygen species; oxidative stress; free fatty acids; tumor necrosis factor-α; fatty acid β-oxidation; NADPH oxidase; intertissue communication;

pathway analysis

1. Introduction

Insulin resistance and obesity are generally brought about by an excessive nutrient condition, attributable to an imbalance among energy intake, expenditure, and storage. Importantly, liver and adipose tissue jointly participate in maintaining glucose and lipid homeostasis through the secretion of various humoral factors and/or neural networks [1-3]. Previous studies have validated the presence of molecular signatures typical of the liver and adipose tissue in mouse models of obesity [4] and in mice fed a high-fat diet (HFD) [5]. It is believed that perturbations in these 'intertissue communications' may be involved in the development of insulin resistance, obesity, and other features of metabolic syndrome [6]. It remains unclear however, which factors alter communication among tissues and impair the ability of tissues to adapt to changing metabolic states.

To determine which initial events trigger the development of HFD-induced insulin resistance and obesity, we globally analyzed the biological pathways that are coordinately altered in both the liver and adipose tissue of mice fed a HFD. This was accomplished through the use of microarray and quantitative real-time PCR analyses. We found that oxidative stress pathways, which are regulated through the balance of ROS production and antioxidant enzyme activity [7], are up-regulated in both tissues prior to the onset of insulin resistance and obesity induced by a HFD.

2. Materials and methods

2.1. Animals and experimental design.

Male C57BL/6J mice were purchased from Charles River Laboratories Japan (Yokohama, Japan) at 6 weeks of age. After a 2-week acclimation period, the mice were divided randomly into two groups: (a) mice given a standard chow containing 5.9% fat (in the form of soybean oil) by weight (control, n = 10), and (b) mice given a high-fat diet containing 60% fat (in the form of cocoa butter) by weight (HFD, n = 10). Both diets used in this study were prepared by Oriental Yeast (Tokyo, Japan). The mice were housed in a room maintained at a controlled temperature (23 ± 1°C) and a 12-h light/12-h dark cycle. In addition, animals were given free access to water and food. All animal procedures were in accordance with the Guidelines for the Care and Use of Laboratory Animals at the Takara-machi campus of Kanazawa University, Japan.

2.2. Glucose and insulin tolerance tests.

For the oral glucose tolerance test (GTT), mice were fasted for 12 h before glucose was

administered at 1.5 g/kg body weight. For the insulin tolerance test (ITT), mice were injected intraperitoneally with insulin (0.5 U/kg body weight, Humulin R; Eli Lilly Japan, Kobe, Japan) following a 4-h fast. Glucose values were measured in whole venous blood using a blood glucose monitoring system (FreeStyle; Kissei, Matsumoto, Japan) at 0, 15, 30, 60, and 120 min after the administration of either glucose or insulin.

2.3. Tissue preparation, blood sampling, and analysis.

Following a 12-h fast, blood samples were obtained from the tail vein. Mice were then sacrificed by cervical dislocation under diethyl ether anesthesia. The liver and adipose tissue (retroperitoneal fat) were immediately removed and weighed. A large portion of tissue was snap-frozen in liquid nitrogen for later RNA analysis. Enzymatic assays for total cholesterol, FFAs, and triglycerides were performed using commercial kits purchased from Wako (Osaka, Japan). The plasma level of TNF-α was measured with a mouse TNF-α ELISA kit (Pierce Biotechnology, Rockford, IL).

2.4. Measurement of hepatic lipid content.

Hepatic lipids were extracted with chloroform:methanol (2:1) according to previously published methods [8]. The resulting extract was dissolved in water and subsequently analyzed for triglycerides, total cholesterol, and FFAs using commercial kits (Wako).

2.5. Measurement of oxidative stress in liver and adipose tissue.

The concentration of proteins containing carbonyl groups in the liver and retroperitoneal fat (those which react with 2,4-dinitrophenylhydrazine to form the corresponding hydrazone) was determined spectrophotometrically according to commercial kit instructions (protein carbonyl assay kit; Cayman Chemical, Ann Arbor, MI).

2.6. RNA preparation for microarray and hybridization analysis.

Total RNA was isolated from the frozen liver and retroperitoneal fat using a ToTALLY RNA kit (Applied Biosystems, Foster City, CA) and a RNeasy Lipid Tissue Mini kit (Qiagen, Germantown, MD), respectively. Each sample was prepared by pooling equal amounts of total RNA from three mice of the same experimental or control group. Three micrograms of total RNA were used for the

synthesis of amino allyl antisense RNA with an Amino Allyl MessageAmp II aRNA kit (Applied Biosystems). These samples were then used for oligo-microarrays (AceGene Mouse 30K, DNA Chip Research, Yokohama, Japan). The microarray hybridization sample and reference antisense RNA were labeled with Cy5 and Cy3, respectively. Hybridization and washing were performed according to the manufacturer's instructions. The microarray was scanned using a G2505B microarray scanner (Agilent Technologies, Palo Alto, CA), and the image was analyzed using GenePix Pro 4.1 software (Axon Instruments, Union City, CA). An arbitrary cut-off signal value (<50) for both colors was used to filter genes with low expression values. Data were normalized (LOWESS method) using GeneSpring v7.2 software (Agilent Technologies). For pathway analysis, we used the GenMAPP and MAPPFinder software packages [9]. The GenMAPP program contains many pathway maps that can be associated with imported microarray data. The MAPPFinder program, which links gene expression data to the pathway maps, can calculate the z score (standardized difference score) and the percentage of genes measured that meet user-defined criteria (±20% in change-fold in our analysis). Using the z score and the percentage, the pathways were ranked by the relative amount of gene expression changes.

2.7. Quantitative real-time PCR.

Total RNA (100 ng of the same sample used for microarray analysis) was reverse transcribed using random primers and SuperScript II reverse transcriptase (Invitrogen, Carlsbad, CA). PCR was performed on an ABI PRISM 7900HT (Applied Biosystems). The specific PCR primers and TaqMan probes were obtained from Applied Biosystems. The PCR conditions were one cycle at 50°C for 2 min and 95°C for 10 min, followed by 40 cycles at 95°C for 15 s and 60°C for 1 min.

2.8. Statistical analysis.

All results are reported as means ± SD. Between-group differences in continuous variables were assessed by univariate analysis using Student's *t*-test. All calculations were performed with SPSS version 12.0 (SPSS, Chicago, IL, USA).

3. Results

3.1. Effects of the HFD on metabolic parameters

As shown in Table 1, no differences were observed in any parameters between the HFD and control mice after 6 weeks of treatment. After 24 weeks, mice fed the HFD weighed significantly more and had more visceral fat compared with control mice. Fasting plasma insulin levels were significantly higher in mice fed the HFD than in control mice. The HFD also induced the accumulation of FFAs in the liver after 24 weeks. These results suggest that mice fed the HFD maintained metabolic homeostasis up to 6 weeks, at which point obesity and insulin resistance developed.

3.2. Effects of the HFD on insulin sensitivity

To evaluate insulin sensitivity, GTT and ITT were conducted after 6 and 24 weeks of treatment in both groups (Fig. 1). Although there was no significant difference in the blood glucose level between the HFD and control mice at 6 weeks, the HFD mice exhibited impaired glucose

tolerance (Fig. 1A) and insulin resistance (Fig. 1B) at 24 weeks. These results are consistent with the above observation that obesity, abdominal adiposity, and hyperinsulinemia were induced only after mice were fed the HFD for 24 weeks.

3.3. Fatty acid metabolism pathways are differentially regulated in liver and adipose tissue of mice fed the HFD

We compared liver and adipose tissue gene expression data between mice fed the HFD and control mice after 6 weeks of treatment to identify pathways with the potential to induce insulin resistance (Table 2). The gene expression levels of various metabolic pathways were already altered at 6 weeks. In particular, pathways for SREBP-1c-related fatty acid synthesis (Fig. 2 and Supplementary Fig. 1A) and PPARα-related fatty acid oxidation were up-regulated in the liver of the HFD mice. In contrast, the pathway for fatty acid synthesis was down-regulated in the adipose tissue (Supplementary Fig. 1B). Such compensatory alterations in the expression of genes that regulate fatty acid metabolism seem to help maintain plasma and hepatic levels of FFAs, which have been considered to be a causal factor for insulin resistance [10, 11]. In the current study, these levels were similar between the HFD mice and control mice at 6 weeks (Table 1).

3.4. Oxidative stress pathways are coordinately up-regulated in both liver and adipose tissue of mice fed the HFD

In contrast to the pathways for fatty acid metabolism, oxidative stress pathways were coordinately up-regulated in both the liver and adipose tissue (Table 2, Supplementary Fig. 1C, D). The oxidative stress pathway is composed of genes for ROS production, stress signaling, and antioxidant enzymes. ROS are radical forms of oxygen that can arise from several biochemical reactions: (1) loading of excessive electrons in the respiratory chain by increased mitochondrial fatty acid β-oxidation [12], (2) peroxisomal fatty acid β-oxidation by acyl-CoA oxidase (Acox) [13], (3) microsomal fatty acid ω-oxidaiton by cytochrome P450 2E1 (CYP2E1) [14], and (4) reduction of oxygen by the Nox complex [15].

To determine the sources of ROS in the liver and adipose tissue of mice fed the HFD, we examined the mRNA expression levels of genes involved in ROS production through the use of quantitative real-time PCR (Fig. 2). In the liver of mice fed a HFD for 6 weeks, the expression levels of genes encoding key regulators of mitochondrial fatty acid β-oxidation, including PPARα, carnitine palmitoyltransferase 1a (CPT-1a), Acox1, and CYP2E1, were significantly up-regulated (1.6-, 2.0-, 1.5-, and 1.5-fold, respectively) compared with control mice, whereas the expression levels of Nox2, Nox4, and the Nox complex components $p22^{phox}$ and $p47^{phox}$ were similar between HFD mice and

control mice. In the adipose tissue of mice fed a HFD for 6 weeks, gene expression levels of Acox1, CYP2E1, Nox4, and $p22^{phox}$ were significantly up-regulated (1.6-, 1.4-, 2.3-, and 1.6-fold, respectively) compared with control mice; in contrast to the liver, the adipose tissue did not show up-regulated expression of the genes for PPARα and CPT-1a. These results suggest that the source of ROS may differ according to the specific tissue, such that a HFD may induce ROS production in distinctly different manners in the liver and adipose tissue. A HFD may induce ROS production through fatty acid oxidation in the mitochondria of the liver but via Nox in the adipose tissue.

Oxidative stress is regulated by the balance between ROS production and antioxidant enzyme activity (7). Consequently, we determined the expression levels of the genes for glutathione peroxidase (Gpx) and Mn-superoxide dismutase (Mn-SOD), both of which reduce ROS and lipid peroxides, resulting in decreased oxidative stress (Fig. 2). The expression level of the Gpx1 gene was significantly up-regulated (3.4-fold) in the adipose tissue, but not in the liver, of mice fed the HFD compared with control mice. The insufficient up-regulation of antioxidant enzymes may therefore cause more oxidative stress in the liver than in the adipose tissue.

The proinflammatory cytokine TNF-α, which is elevated in obese rodents and humans, is also an important contributor to the development of insulin resistance [16]. However, the mRNA expression level of TNF-α in the liver and adipose tissue of mice fed the HFD for 6 weeks was similar

to that of control mice (Fig. 2). Furthermore, the plasma level of TNF-α was below the detection limit of the ELISA (<10 pg/mL) in both groups. These results suggest that the up-regulation of genes for ROS production, rather than the elevation of TNF-α, may be an early event triggering insulin resistance in mice fed a HFD.

3.5. Evaluation of oxidative stress in the liver and adipose tissue of mice fed the HFD

To confirm whether high fat intake increases oxidative stress, we measured the protein carbonyl level (marker for cumulative oxidative stress) in the liver and adipose tissue. As expected, the protein carbonyl level was elevated by 35% in the liver but was not altered in the adipose tissue of mice fed the HFD compared with control mice at 6 weeks (Fig. 3). The up-regulation of antioxidant enzymes (*i.e.*, Gpx1) in the adipose tissue may compensate for the increase of ROS, lowering oxidative stress.

4. Discussion

ROS production is one of many factors that have been suggested to play a role in the development of insulin resistance, based on the following evidence: (1) high doses of hydrogen peroxide [17] and reagents that accumulate ROS [18] can induce insulin resistance in 3T3-L1 adipocytes, and (2) increased markers of oxidative stress were observed in obese humans [19] and rodents [17, 20]. It remains unclear, however, whether increased ROS production causes insulin resistance *in vivo*. In this study, we demonstrated that the up-regulation of genes responsible for ROS production occurs in both the liver and adipose tissue prior to the onset of insulin resistance and obesity in mice fed a HFD.

In our dietary model of insulin resistance, the mRNA up-regulation of genes for fatty acid oxidation was observed in the liver. Previous studies have also shown that fatty acid oxidation was increased in the liver to compensate for high fat intake [21]. In addition, pathways involved in the mitochondrial respiratory chain were coordinately down-regulated in both the liver and adipose tissue of mice fed the HFD. These results are consistent with previous reports in skeletal muscle of both humans and mice [22]. High mitochondrial β-oxidation rates seem to help metabolize excess FFAs, although large amounts of electrons entering the respiratory chain may cause abnormal reduction of oxygen. An influx of electrons may then lead to increased mitochondrial ROS production. This

suggests that impaired respiratory chain function may cause increased mitochondrial ROS production. Furthermore, we speculate that the down-regulation of the respiratory chain may lead to an influx of FFAs to intracellular peroxisomes and microsomes instead of to mitochondria, resulting in further generation of ROS by Acox and CYP2E1, genes up-regulated in both liver and adipose tissue in this study.

The Nox complex may be a major source of ROS production in adipose tissue but not in liver. Furukawa *et al.*[17] reported that the mRNA expression of Nox2 and its subunits $p22^{phox}$, $p47^{phox}$, and $p67^{phox}$ was significantly up-regulated in the adipose tissue of obese KKAy mice compared with lean C57BL/6J mice. In the present study, however, the HFD up-regulated only Nox4 and $p22^{phox}$ expression in adipose tissue. This discrepancy may be attributed to the difference between genetically and HFD-induced obese models. Given that complexes of Nox4 with $p22^{phox}$ increase in the kidney of diabetic rats [23], excessive nutrients (*e.g.*, high fat intake) may also induce ROS production via the Nox4/$p22^{phox}$ complex.

It is striking that increased ROS production preceded the elevated levels of TNF-α and FFAs in the plasma and liver. Although TNF-α and FFAs are thought to cause insulin resistance, our results raise the possibility that ROS trigger the development of insulin resistance, resulting in abdominal obesity and elevated TNF-α and FFAs. In summary, the HFD induced oxidative stress,

potentially through the up-regulated expression of genes for ROS production, in the liver and adipose tissue. In addition, these changes occurred prior to the onset of insulin resistance and obesity. Sources of ROS induced by a HFD may differ between the liver and adipose tissue. These findings suggest that ROS production may be the initial event triggering HFD-induced insulin resistance and therefore may be an attractive therapeutic target for preventing insulin resistance and obesity caused by a HFD.

Acknowledgements

We thank A. Katayama and M. Nakamura for technical assistance.

References

［1] Yamauchi T, Kamon J, Minokoshi Y, Ito Y, Waki H, Uchida S, Yamashita S, et al. Adiponectin stimulates glucose utilization and fatty-acid oxidation by activating AMP-activated protein kinase. Nat Med 2002;8:1288-1295.

[2] Watanabe M, Houten SM, Mataki C, Christoffolete MA, Kim BW, Sato H, Messaddeq N, et al. Bile acids induce energy expenditure by promoting intracellular thyroid hormone activation. Nature 2006;439:484-489.

[3] Uno K, Katagiri H, Yamada T, Ishigaki Y, Ogihara T, Imai J, Hasegawa Y, et al. Neuronal pathway from the liver modulates energy expenditure and systemic insulin sensitivity. Science 2006;312:1656-1659.

[4] Lan H, Rabaglia ME, Stoehr JP, Nadler ST, Schueler KL, Zou F, Yandell BS, et al. Gene expression profiles of nondiabetic and diabetic obese mice suggest a role of hepatic lipogenic capacity in diabetes susceptibility. Diabetes 2003;52:688-700.

[5] Gregoire FM, Zhang Q, Smith SJ, Tong C, Ross D, Lopez H, West DB. Diet-induced obesity and hepatic gene expression alterations in C57BL/6J and ICAM-1-deficient mice. Am J Physiol Endocrinol Metab 2002;282:E703-713.

[6] Herman MA, Kahn BB. Glucose transport and sensing in the maintenance of glucose homeostasis

and metabolic harmony. J Clin Invest 2006;116:1767-1775.

[7] Nordberg J, Arner ES. Reactive oxygen species, antioxidants, and the mammalian thioredoxin system. Free Radic Biol Med 2001;31:1287-1312.

[8] Folch J, Lees M, Sloane Stanley GH. A simple method for the isolation and purification of total lipides from animal tissues. J Biol Chem 1957;226:497-509.

[9] Doniger SW, Salomonis N, Dahlquist KD, Vranizan K, Lawlor SC, Conklin BR. MAPPFinder: using Gene Ontology and GenMAPP to create a global gene-expression profile from microarray data. Genome Biol 2003;4:R7.

[10] Boden G. Role of fatty acids in the pathogenesis of insulin resistance and NIDDM. Diabetes 1997;46:3-10.

[11] Boden G, She P, Mozzoli M, Cheung P, Gumireddy K, Reddy P, Xiang X, et al. Free fatty acids produce insulin resistance and activate the proinflammatory nuclear factor-kappaB pathway in rat liver. Diabetes 2005;54:3458-3465.

[12] St-Pierre J, Buckingham JA, Roebuck SJ, Brand MD. Topology of superoxide production from different sites in the mitochondrial electron transport chain. J Biol Chem 2002;277:44784-44790.

[13] Osmundsen H, Bremer J, Pedersen JI. Metabolic aspects of peroxisomal beta-oxidation. Biochim Biophys Acta 1991;1085:141-158.

[14] Chitturi S, Farrell GC. Etiopathogenesis of nonalcoholic steatohepatitis. Semin Liver Dis 2001;21:27-41.

[15] Krieger-Brauer HI, Kather H. Human fat cells possess a plasma membrane-bound H2O2-generating system that is activated by insulin via a mechanism bypassing the receptor kinase. J Clin Invest 1992;89:1006-1013.

[16] Hotamisligil GS, Shargill NS, Spiegelman BM. Adipose expression of tumor necrosis factor-alpha: direct role in obesity-linked insulin resistance. Science 1993;259:87-91.

[17] Furukawa S, Fujita T, Shimabukuro M, Iwaki M, Yamada Y, Nakajima Y, Nakayama O, et al. Increased oxidative stress in obesity and its impact on metabolic syndrome. J Clin Invest 2004;114:1752-1761.

[18] Lin Y, Berg AH, Iyengar P, Lam TK, Giacca A, Combs TP, Rajala MW, et al. The hyperglycemia-induced inflammatory response in adipocytes: the role of reactive oxygen species. J Biol Chem 2005;280:4617-4626.

[19] Urakawa H, Katsuki A, Sumida Y, Gabazza EC, Murashima S, Morioka K, Maruyama N, et al. Oxidative stress is associated with adiposity and insulin resistance in men. J Clin Endocrinol Metab 2003;88:4673-4676.

[20] Diniz YS, Rocha KK, Souza GA, Galhardi CM, Ebaid GM, Rodrigues HG, Novelli Filho JL, et

al. Effects of N-acetylcysteine on sucrose-rich diet-induced hyperglycaemia, dyslipidemia and oxidative stress in rats. Eur J Pharmacol 2006;543:151-157.

[21] Akbiyik F, Cinar K, Demirpence E, Ozsullu T, Tunca R, Haziroglu R, Yurdaydin C, et al. Ligand-induced expression of peroxisome proliferator-activated receptor alpha and activation of fatty acid oxidation enzymes in fatty liver. Eur J Clin Invest 2004;34:429-435.

[22] Sparks LM, Xie H, Koza RA, Mynatt R, Hulver MW, Bray GA, Smith SR. A high-fat diet coordinately downregulates genes required for mitochondrial oxidative phosphorylation in skeletal muscle. Diabetes 2005;54:1926-1933.

[23]Etoh T, Inoguchi T, Kakimoto M, Sonoda N, Kobayashi K, Kuroda J, Sumimoto H, et al. Increased expression of NAD(P)H oxidase subunits, NOX4 and p22phox, in the kidney of streptozotocin-induced diabetic rats and its reversibity by interventive insulin treatment. Diabetologia 2003;46:1428-1437.

Figure Legends

Fig. 1. Evaluation of glucose tolerance and insulin sensitivity.

GTT (A) and ITT (B) after 6 or 24 weeks of standard chow or the HFD. Values represent the means ± SD for five mice. *$P < 0.05$ versus the control group.

Fig. 2. Quantitative real-time PCR for representative genes involved in fatty acid metabolism and oxidative stress.

The mRNA levels of SREBP-1c, Fatty acid synthase, PPARα, CPT-1a, Acox1, CYP2E1, Nox2, Nox4, $p22^{phox}$, $p47^{phox}$, Gpx1, Mn-SOD, and TNF-α in the liver or retroperitoneal fat of mice fed standard chow ($n = 3$) or the HFD ($n = 3$) were quantified using real-time PCR after 6 weeks of feeding. The RNA samples for real-time PCR were the same as those for the microarray analysis. Gene expression levels were normalized to 18S rRNA. The degree of change in gene expression is based on the mean expression level of control mice. Values represent the means ± SD for three mice. *$P < 0.05$ and **$P < 0.01$ versus the control mice.

Fig. 3. Measurement of protein carbonyl levels in the liver and adipose tissue.

Protein carbonyl concentration was analyzed as a marker for oxidative stress in the liver and

retroperitoneal fat. Values represent the means ± SD for five mice. *$P < 0.05$ versus the control mice.

Table 1. Clinical and biochemical parameters of mice fed the standard chow or high-fat diet (HFD) after 6 or 24 weeks.

	6 weeks		24 weeks	
Diet type	control	HFD	control	HFD
Body weight (g)	25.1±0.9	26.5±1.4	29.0±1.5	35.2±3.8*
Liver weight (g)	1.11±0.09	1.03±0.12	1.28±0.07	1.20±0.23
Retroperitoneal fat pad weight (g)	0.07±0.05	0.10±0.08	0.24±0.09	0.61±0.17**
Plasma triglycerides (mg/dL)	69.1±9.0	75.0±18.9	41.5±9.2	63.0±15.0
Plasma total cholesterol (mg/dL)	85.0±7.4	117.7±37.0	84.6±7.9	132.6±26.1*
Plasma FFAs (mEq/L)	0.60±0.16	0.61±0.21	0.48±0.09	0.54±0.16
Plasma TNF-α (pg/mL)	<10	<10	N.D.	N.D.
Fasting plasma insulin (μU/mL)	14.6±3.6	18.1±7.6	15.7±6.2	43.3±14.3*
Hepatic triglycerides (μg/mg protein)	64.8±23.2	73.8±15.4	148.6±46.7	143±43.0
Hepatic total cholesterol (μg/mg protein)	43.0±6.3	40.8±6.0	34.3±4.9	36.5±4.5
Hepatic FFAs (μEq/mg protein)	46.7±6.9	48.8±3.6	53.1±4.0	71.0±7.6*

Values represent the means ± SD of 5 mice per group. FFAs, free fatty acids. N.D., not determined. Significantly different from control value: *, $p < 0.05$; **, $p < 0.01$.

Table 2. Biological pathways of liver or adipose tissue genes regulated by the HFD after 6 weeks

Pathway name	Number of genes changed	Number of genes measured	z score	permuted *P* value
Liver				
Up-regulated				
Cholesterol biosynthesis	10	15	4.61	< 0.001
Fatty acid synthesis	9	14	4.23	< 0.001
Oxidative stress	16	38	3.52	0.001
Glucocorticoid mineralocorticoid metabolism	7	12	3.39	0.006
Statin pathway	9	19	3.06	0.005
Glycolysis and gluconeogenesis	14	41	2.37	0.018
Fatty acid beta oxidation	10	27	2.30	0.021
Down-regulated				
Electron transport chain (= respiratory chain)	28	82	4.77	< 0.001
ACE-inhibitor pathway	5	8	3.72	0.003
Adipose tissue				
Up-regulated				
TGF Beta signaling pathway	27	50	3.645	0.001
Complement and coagulation cascades	29	59	3.149	0.001
Adipogenesis	51	129	2.638	0.014
Oxidative stress	18	38	2.287	0.026
Smooth muscle contraction	61	157	2.282	0.024
Inflammatory response pathway	18	40	2.018	0.037
Down-regulated				
Focal adhesion	74	189	3.50	< 0.001
Glycolysis and gluconeogenesis	21	41	3.35	< 0.001
Electron transport chain (= respiratory chain)	35	82	3.01	0.002
Krebs-TCA cycle	14	29	2.46	0.020
Fatty acid synthesis	8	14	2.45	0.029
Pentose phosphate pathway	5	8	2.19	0.038

Pathway analysis was performed using MAPPFinder 2.0 and the Mm-std 20051114.gdb data base. The criteria for genes with significantly increased or decreased expression were change-fold (ratio to control) >20% (i.e. >1.20 or <0.83). For each pathway, the number of genes that meet the criteria for a significant increase or decrease was determined. This number was compared with the number pathway genes detected by microarray analysis. These value were used to calculate of z score and the permuted *P* value. Pathways indicated by arrows were coordinately regulated between in the liver and adipose tissue (retroperitoneal fat). On the other hand, pathways for fatty acid synthesis and glycolysis and gluconeogenesis were up-regulated in the liver (highlighted in red) and down-regulated in adipose tissue (highlighted in green).

Figure 1

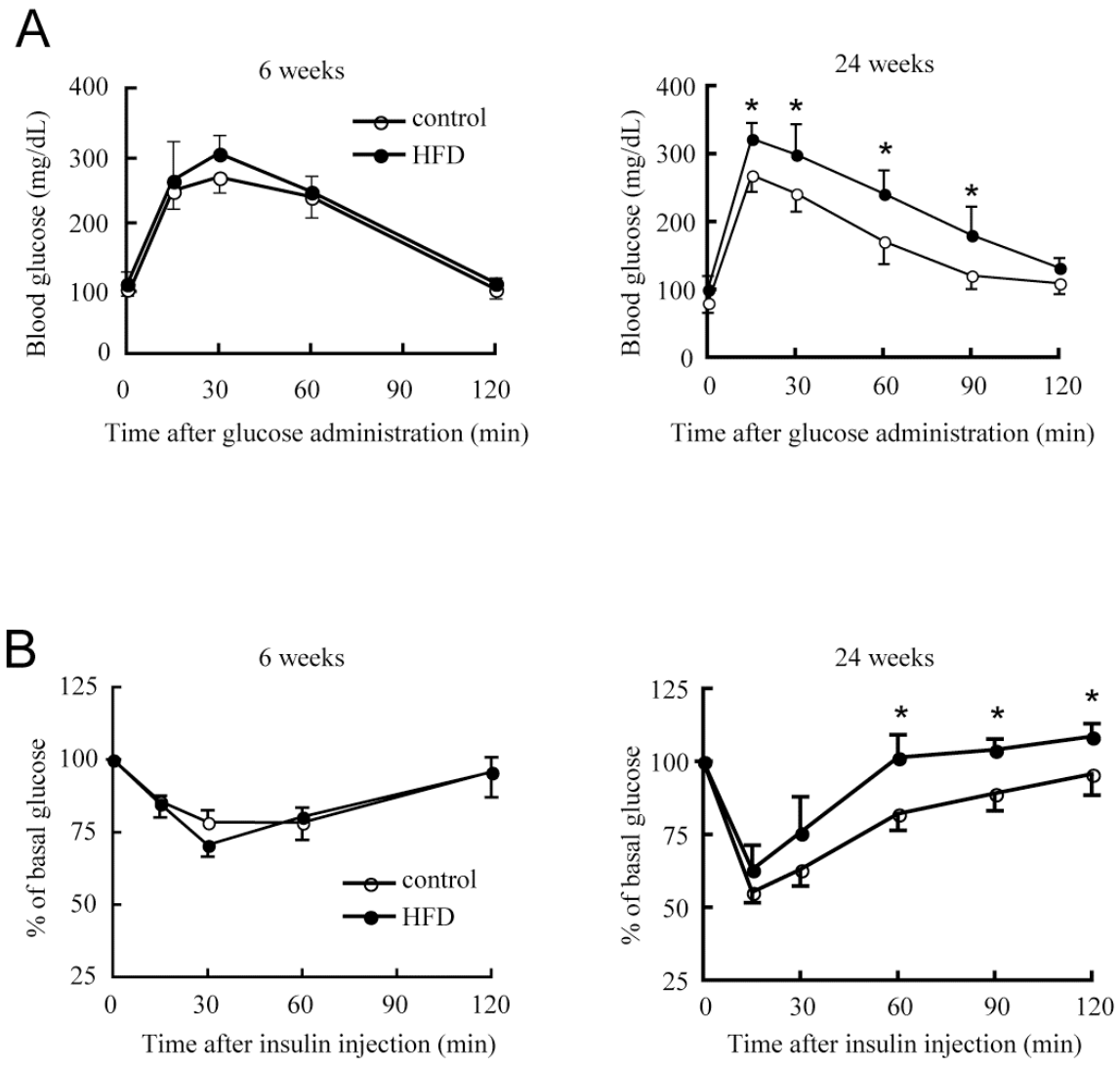
A
6 weeks
24 weeks
Blood glucose (mg/dL)
400
300
200
100
0
control
HFD
*
0
30
60
90
120
Time after glucose administration (min)
B
% of basal glucose
125
100
75
50
25
Time after insulin injection (min)

Figure 2

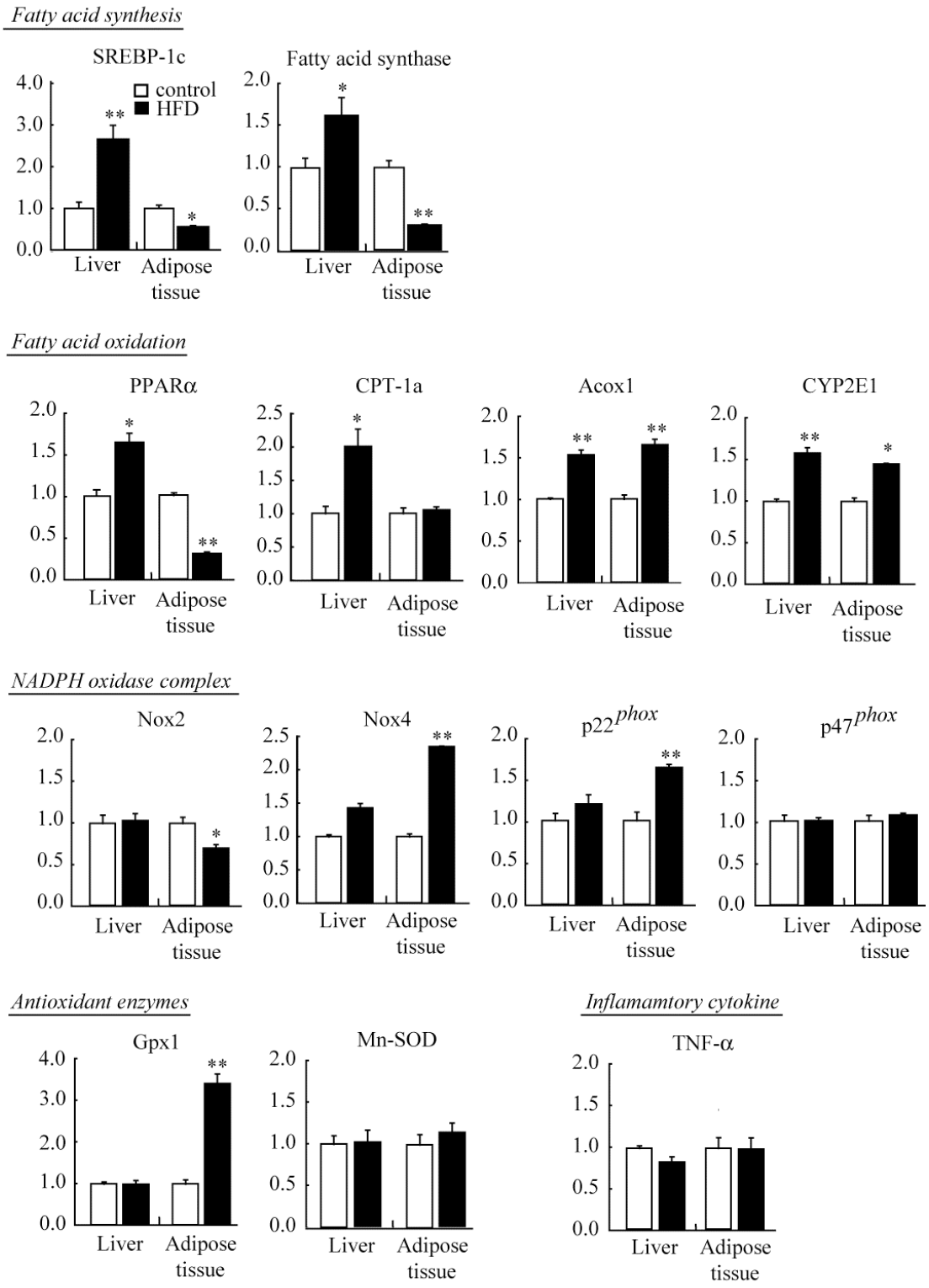
Fatty acid synthesis
SREBP-1c
control
HFD
Fatty acid synthase
Liver
Adipose tissue
Fatty acid oxidation
PPARα
CPT-1a
Acox1
CYP2E1
NADPH oxidase complex
Nox2
Nox4
p22phox
p47phox
Antioxidant enzymes
Gpx1
Mn-SOD
Inflamamtory cytokine
TNF-α

Figure 3

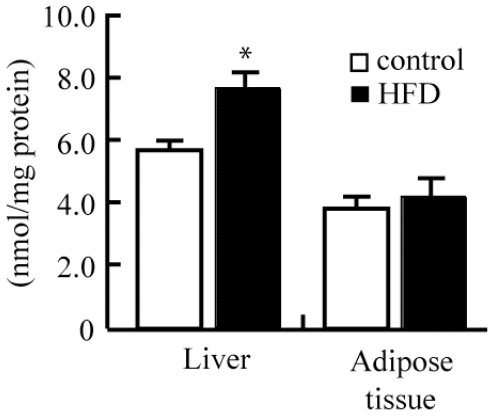
10.0
8.0
6.0
4.0
2.0
0
(nmol/mg protein)
*
control
HFD
Liver
Adipose tissue

Legends for supplementary figure

Supplementary Fig. 1. Illustration of the pathways for fatty acid synthesis and oxidative stress in the liver and adipose tissue. The genes involved in fatty acid synthesis were up-regulated in the liver of mice fed a HFD (A), whereas they were down-regulated in the adipose tissue (B). However, the genes involved in oxidative stress were coordinately up-regulated in both the liver (C) and retroperitoneal fat (D) of mice fed the HFD. Each pathway is adapted from a view in GenMAPP. The fold change presented beside the name of each gene is for mice fed the HFD compared with control mice. Genes up-regulated more than 1.2-fold or 2.0-fold by HFD are colored pink or red, respectively. Genes down-regulated more than 1.2-fold or 2.0-fold by HFD are colored pale green or green, respectively. Genes analyzed but not altered in mice fed the HFD are colored gray.

Supplementary Figure 1

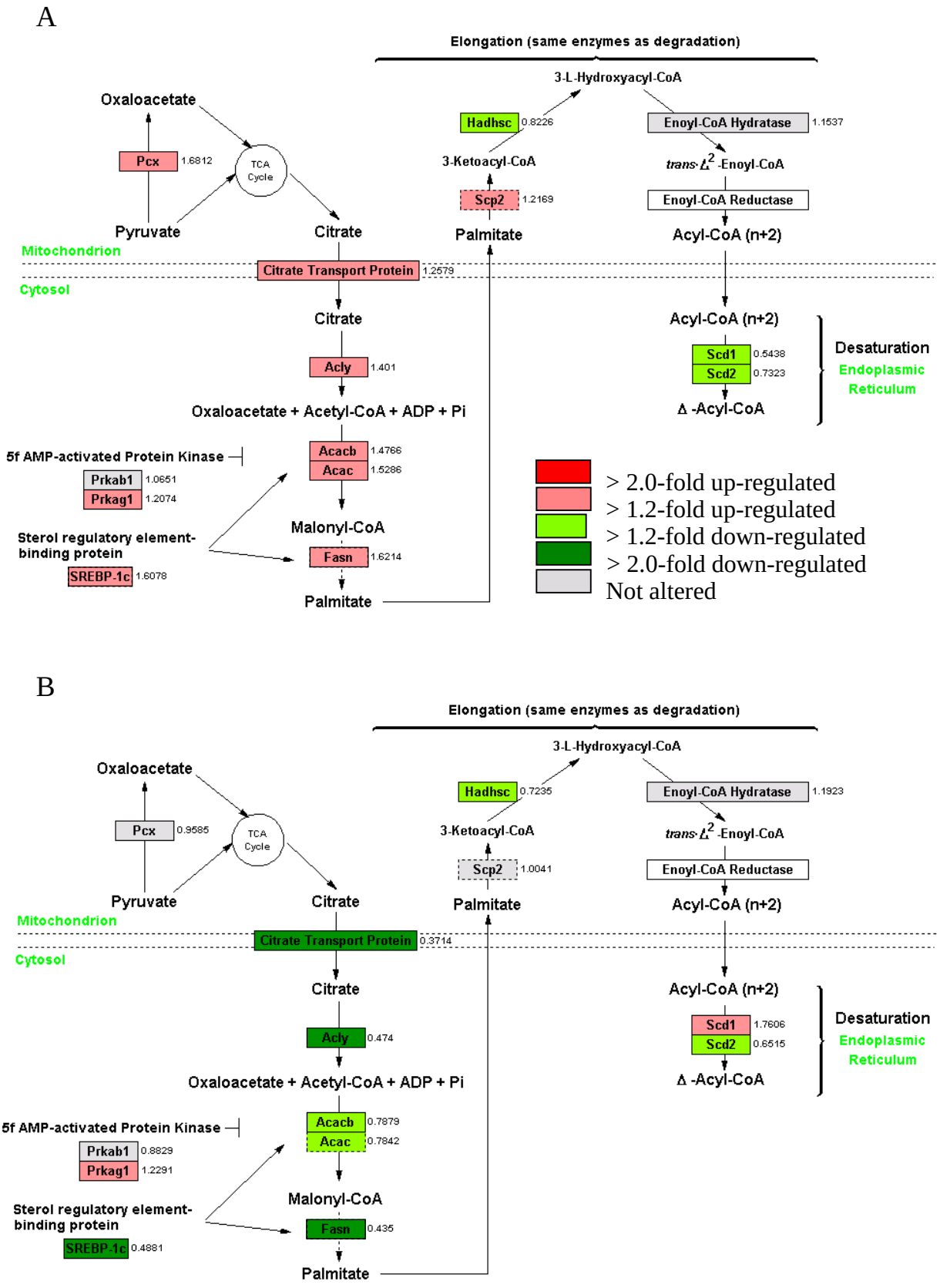

C

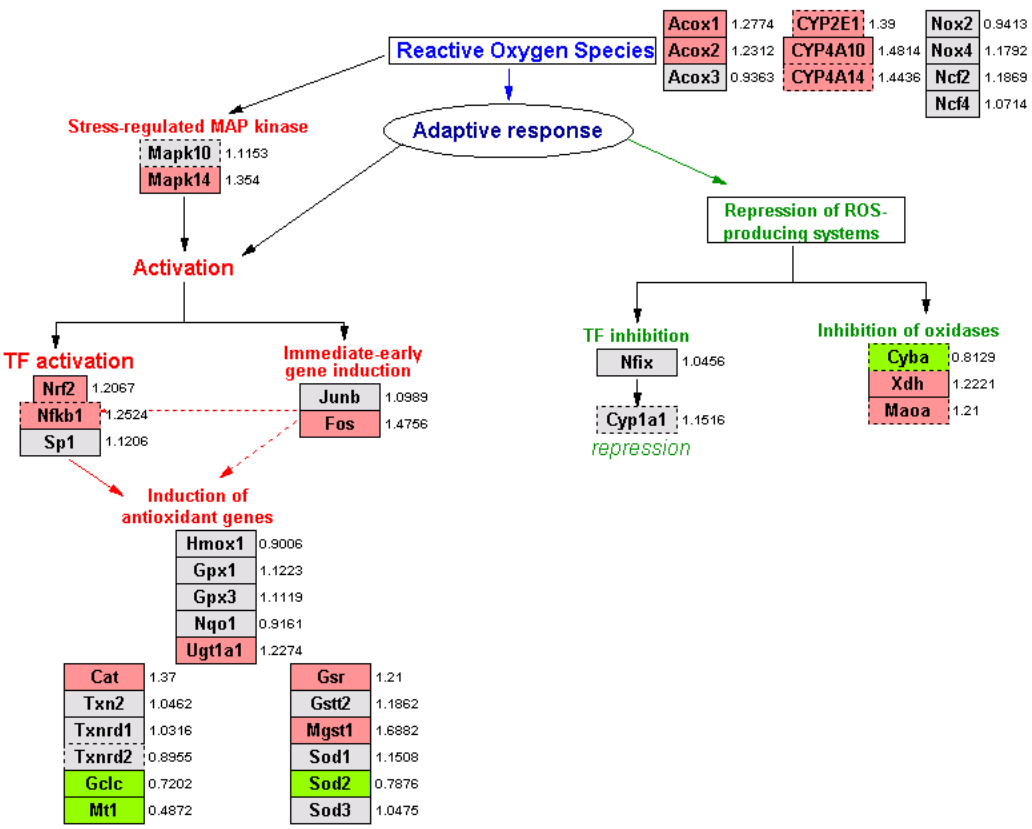
Reactive Oxygen Species
Acox1 1.2774
Acox2 1.2312
Acox3 0.9363
CYP2E1 1.39
CYP4A10 1.4814
CYP4A14 1.4436
Nox2 0.9413
Nox4 1.1792
Ncf2 1.1869
Ncf4 1.0714
Stress-regulated MAP kinase
Mapk10 1.1153
Mapk14 1.354
Adaptive response
Repression of ROS-producing systems
Activation
TF activation
Nrf2 1.2067
Nfkb1 1.2524
Sp1 1.1206
Immediate-early gene induction
Junb 1.0989
Fos 1.4756
TF inhibition
Nfix 1.0456
Cyp1a1 1.1516
repression
Inhibition of oxidases
Cyba 0.8129
Xdh 1.2221
Maoa 1.21
Induction of antioxidant genes
Hmox1 0.9006
Gpx1 1.1223
Gpx3 1.1119
Nqo1 0.9161
Ugt1a1 1.2274
Cat 1.37
Txn2 1.0462
Txnrd1 1.0316
Txnrd2 0.8955
Gclc 0.7202
Mt1 0.4872
Gsr 1.21
Gstt2 1.1862
Mgst1 1.6882
Sod1 1.1508
Sod2 0.7876
Sod3 1.0475

D

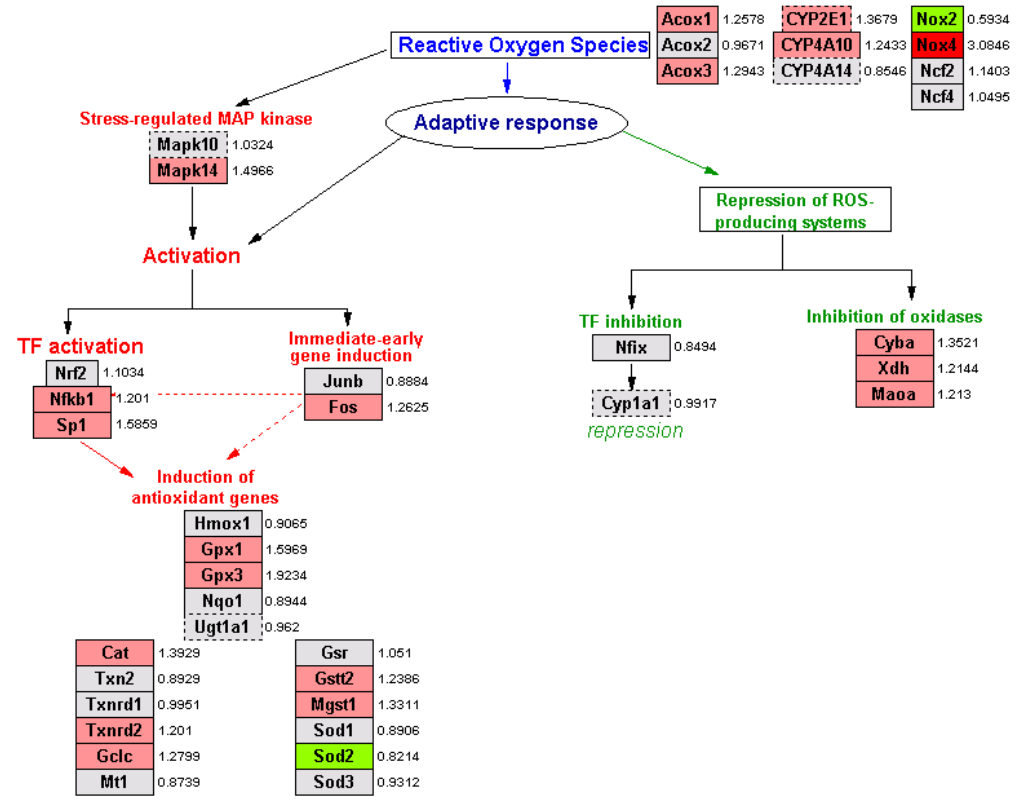
Reactive Oxygen Species
Acox1 1.2578
Acox2 0.9671
Acox3 1.2943
CYP2E1 1.3679
CYP4A10 1.2433
CYP4A14 0.8546
Nox2 0.5934
Nox4 3.0846
Ncf2 1.1403
Ncf4 1.0496
Stress-regulated MAP kinase
Mapk10 1.0324
Mapk14 1.4966
Adaptive response
Repression of ROS-producing systems
Activation
TF activation
Nrf2 1.1034
Nfkb1 1.201
Sp1 1.5859
Immediate-early gene induction
Junb 0.8884
Fos 1.2625
TF inhibition
Nfix 0.8494
Cyp1a1 0.9917
repression
Inhibition of oxidases
Cyba 1.3521
Xdh 1.2144
Maoa 1.213
Induction of antioxidant genes
Hmox1 0.9065
Gpx1 1.5969
Gpx3 1.9234
Nqo1 0.8944
Ugt1a1 0.962
Cat 1.3929
Txn2 0.8929
Txnrd1 0.9951
Txnrd2 1.201
Gclc 1.2799
Mt1 0.8739
Gsr 1.051
Gstt2 1.2386
Mgst1 1.3311
Sod1 0.8906
Sod2 0.8214
Sod3 0.9312